



Published in final edited form as:

Mol Cancer Res. 2021 May ; 19(5): 823–833. doi:10.1158/1541-7786.MCR-20-0721.

Colorectal cancer-associated Smad4 R361 hotspot mutations boost Wnt/ β -catenin signaling through enhanced Smad4-LEF1 binding

Claudia B. Lanauze^{1,6}, Priyanka Sehgal¹, Katharina Hayer^{1,3}, Manuel Torres-Diz¹, James A Pippin², Struan F A Grant^{2,4}, Andrei Thomas-Tikhonenko^{1,4,5,*}

¹Division of Pathobiology, Children's Hospital of Philadelphia

²Division of Human Genetics, Children's Hospital of Philadelphia

³Department of Biomedical & Health Informatics, Children's Hospital of Philadelphia

⁴Department of Pediatrics, Perelman School of Medicine at the University of Pennsylvania, Philadelphia, PA 19104, USA

⁵Department of Pathology & Laboratory Medicine, Perelman School of Medicine at the University of Pennsylvania, Philadelphia, PA 19104, USA

⁶Cell & Molecular Biology Graduate Group, Perelman School of Medicine at the University of Pennsylvania, Philadelphia, PA 19104, USA

Abstract

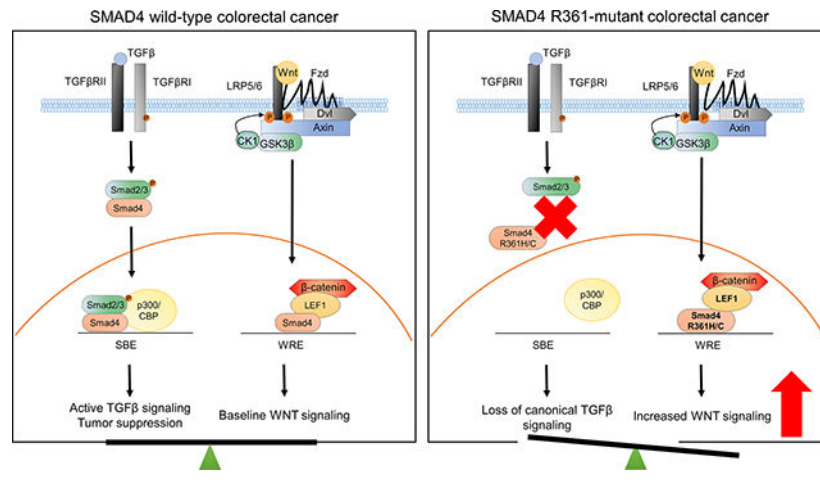
10–30% of colorectal cancer (CRC) patients harbor either loss of or missense mutations in SMAD4, a critical component of the TGF β signaling pathway. The pathophysiological function of missense mutations in Smad4 is not fully understood. They usually map to the MH2 domain, specifically to residues that are involved in heterodimeric complex formation with regulatory Smads (such as Smad2/3) and ensuing transcriptional activation. These detrimental effects suggest that SMAD4 missense mutations can be categorized as loss-of-function. However, they tend to cluster in a few hotspots, which is more consistent with them acting by a gain-of-function mechanism. In this study, we investigated the functional role of Smad4 R361 mutants by re-expressing two R361 Smad4 variants in several Smad4-null CRC cell lines. As predicted, R361 mutations disrupted Smad2/3-Smad4 heteromeric complex formation and abolished canonical TGF β signaling. In that, they were similar to SMAD4 loss. However, RNA sequencing and subsequent RT-PCR revealed that Smad4mut cells acquired a gene signature associated with enhanced Lef1 protein function and increased Wnt signaling. Mechanistically, Smad4 mutant proteins retained binding to Lef1 protein and drove a commensurate increase in downstream Wnt signaling as measured by TOP/FOP luciferase assay and Wnt-dependent cell motility. Consistent with these findings, human CRCs with SMAD4 missense mutations were less likely to acquire activating mutations in the key Wnt pathway gene CTNNB1 (encoding beta catenin) than CRCs with truncating SMAD4 nonsense mutations.

*To whom correspondence should be addressed. Tel: +1 267 426 9699; Fax: +1 267 426 8125; andreit@penmedicine.upenn.edu.

Disclosure of Potential Conflicts of Interest

The authors declare that they have nothing to disclose.

Graphical Abstract



INTRODUCTION.

The transforming growth factor beta (TGFβ) signaling pathway plays an important role in a variety of cellular processes such as cell growth, differentiation, and apoptosis. It is activated by TGFβ ligands, which bring together receptors type I and type II. Upon receptor dimerization, activation of the type I receptor kinase leads to signal propagation by phosphorylation of receptor-regulated Smad 2 and 3, or R-Smads. In the case of TGFβ, phosphorylated Smad2 and/or Smad3 will form a complex with Smad4, a common mediator Smad, which is also involved in other TGFβ superfamily signaling pathways triggered by activins and bone morphogenic proteins (BMPs). Once the complex forms, it translocates into the nucleus, bind to other transcription factors and DNA, and modulate the transcription of target genes (1,2).

In normal and premalignant cells, TGFβ can exert tumor-suppressive effects by inhibiting cell proliferation, stimulating differentiation and inducing apoptosis (3). However, tumor cells can evade TGFβ tumor suppression through inactivation of either the receptors or downstream effectors, which disables the entire signaling cascade. For example, TGFβ RII is frequently mutated in colon carcinoma cells from patients with microsatellite unstable (MSI) CRC, a phenomenon defined by faulty DNA mismatched repair machinery (4). Inactivating mutations in Smads, specifically Smad4, have been found in various types of cancers such as lung and pancreatic carcinomas (5–9) and germ-line mutations are common in juvenile polyposis, a disease which predisposes individuals to gastrointestinal malignancies(10). Smad4 alterations are also found in 10–35% of CRC tumors and tend to appear late in the adenoma-to-carcinoma progression (11,12). Complete loss of Smad4 in colorectal cancer patients can be due to deep deletions or frameshift mutations. We and other have shown that it is frequently associated with increased angiogenesis (13,14), lymph node metastasis, advanced disease, and poor prognosis (15). In addition, many patients acquire missense mutations, which cluster in the MH2 domain of the protein. While mutations in the MH2 domain mainly affect residues close to protein interface involved in hetero-oligomerization of Smad4 with R-Smads which is required for transcriptional activation

(16,17), mutations in the MH1 domain have been shown to alter protein stability and binding to the DNA (18,19). Under either scenario, Smad4 missense mutations are thought to be loss-of-function. However, there is a considerable gap in our understanding of their role in CRC progression and whether these mutant forms of Smad4 retain or acquire any functions.

Here we report that R361 Smad4 variants can function independently of TGF β -signaling and positively regulate Wnt signaling, a pathway often hyperactivated in CRC (20). We demonstrate that mutant Smad4 binds to lymphoid enhancer binding factor-1 (Lef1) protein and facilitates transcriptional activation of Wnt signaling in CRC cells. Overall, we establish a novel function for mutant Smad4 proteins in the progression of colorectal cancer.

MATERIALS AND METHODS

Cell culture and treatments.

Colorectal cancer cell lines SW480, SW620, and HCT116 3:6 cells (Supp Figure S1) were maintained in Dulbecco's modified Eagle's medium (DMEM) containing 10% fetal bovine serum (FBS) and penicillin/streptomycin (p/s) at 37 °C and 5% CO₂. After thawing, cells were used for up to 10–12 passages and their authenticities were verified by short tandem repeat analysis. Cells were tested for Mycoplasma using EZ-PCR Mycoplasma PCR Detection Kit (Biological Industries). For the TGF β treatment experiments, recombinant human TGF β (R&D systems, 240-B-010) was used at a concentration of 5 or 10ng/mL at the indicated time points. Cells were treated with recombinant Wnt3a ligand (R&D systems, 5036-WN) at 100ng/mL at indicated time points.

Transient transfections and retrovirus-mediated gene transfer.

For infection of CRC cell lines with pMX-IRES constructs, retroviral particles were generated by transfection of HEK 293GP cells with Lipofectamine 3000 (Invitrogen). The virus-containing medium was collected after 8 hr or overnight and supplemented with 4 μ g/ml polybrene (Sigma-Aldrich) and 1% FBS. Subsequently, the virus was filtered using 0.45 μ m filter and viral supernatant was added to the target cells for 8 hours to overnight. Selection for infected cells was done with 12.5 μ g/ml Blasticidin (Gemini Bio Products) for over a week.

Plasmid generation.

Plasmid encoding FLAG tagged, human Smad4 (Addgene item # 14039) was first subcloned into pBlueScriptII vector and subsequently cloned into pMX-IRES-Blasticidin (Gemini Bio Products) retroviral vector. R361 Smad4 point mutations were generated using Q5 Site-directed Mutagenesis kit (NEB Cat #) with primers that carry the desired mutation. For LEF1 constructs, FLAG/MYC tagged LEF1 was purchased from Origene (CAT #RC208663). FLAG tag was substituted with an HA tag by using Q5 Site-directed Mutagenesis kit (NEB) according to manufacturer's protocol.

Chromatin Immunoprecipitation (ChIP) qPCR.

SW480 cells (2.0×10^6) were fixed by 1% formaldehyde for 10 min at room temperature and were then quenched by 125 mM glycine for 15 min at room temperature, washed with

ice-cold PBS twice and centrifuged at 200g, 4°C for 5 min. The pellet was resuspended in 1 mL of cell lysis buffer (10 mM Tris-HCl, 10 mM NaCl, 0.5% NP-40, protease inhibitor) and kept at 4°C rotating for 30 min. After centrifugation, the pellet was resuspended in 1 mL of nuclear lysis buffer (1% SDS, 10 mM EDTA, 50 mM Tris-HCl pH 8.0, protease inhibitor) and kept at 4°C for 60 min. Lysate was then sonicated to an average size of chromatin fragments of 0.25–1.00 kb and then frozen at –20°C overnight. The chromatin was thawed on ice and centrifuged at 2,500g for 30 mins. Immunoprecipitation and DNA purification experiments were performed using Chip-It High Sensitivity Kit (Active Motif # 53040) according to manufacturer's protocol. The immunoprecipitated fraction was analyzed by qRT-PCR to determine the abundance of the target DNA sequence(s) relative to normal rabbit IgG control. The PAI-1 primer sequences were GCAGGACATCCGGGAGAGA (forward) and CCAATAGCCTTGGCCTGAGA (reverse), as described in the literature (21).

Luciferase assay.

SW480, SW620, and HCT116 3:6 cells (250,000 per well) were seeded into 12-well plates and rested overnight. Cells were then transiently transfected with SBE4-Luc (Addgene #16495), TOP-FLASH (Addgene #12456) or FOP-FLASH (Addgene #12457) reporter plasmids for 24 hrs, using renilla luciferase as internal control. For TGFβ and Wnt treatments, transfected cells were stimulated with TGFβ or Wnt3a in serum-free media for an additional 24 hrs. Firefly luciferase reporter activity was measured with a dual luciferase reporter assay kit (Promega), according to the manufacturer's protocol. Expression was calculated as the ratio of firefly luciferase units normalized to *renilla* luciferase. These experiments were independently repeated three times and each treatment consisted of triplicate samples.

Western blotting and antibodies.

Whole cell protein lysates were prepared in RIPA buffer (0.15M NaCl, 1% sodium deoxycholate, 0.1% sodium dodecyl sulfate, 1% Triton X-100, 1mM phenylmethylsulfonyl fluoride, 0.05M Tris-HCl, pH 7.4) containing protease and phosphatase inhibitors (Pierce Halt Inhibitor Cocktail, Thermo Scientific). Protein concentrations were estimated by Biorad colorimetric assay (BCA). Bound antibodies were detected with enhanced chemiluminescence (ECL kit, cat #) or by Odyssey Infrared Imager (LI-COR Biosciences). The following primary antibodies were used: Smad4, Smad2, Smad3, phospho-Smad2, phospho-Smad3, Actin, HA (Cell signaling) and FLAG (Sigma-Aldrich). For secondary antibodies, goat anti-rabbit-HRP (GE Healthcare NA934V), goat anti-mouse HRP (GE Healthcare NA931V), goat anti-mouse-680 (Licor 925–32220) donkey anti-rabbit-800 (Licor 926–32213) were used. Dilutions were used according to the recommendation of the respective manufacturers.

CRISPR/Cas9 genome-editing system.

Smad4 CRISPR/Cas9 knockout and homology directed repair plasmids were purchased from Santa Cruz Biotechnologies (sc-400110 and sc-400110-HDR) and transfected into HCT116 3:6 cell lines through Lipofectamine 3000 (per manufacturer's protocol). Effective Smad4 knockdown was confirmed by western blotting.

Co-immunoprecipitation (co-IP).

Cells stably expressing Flag-Smad4 (either wild-type or mutated) were collected and subsequently lysed in lysis buffer (50 mM Tris-HCl at pH 7.5 1M, 150 mM NaCl 5M, 1 mM EDTA, 1% Triton, 0.1% SDS, 0.5% NA-deoxycholate plus protease and phosphatase inhibitors) and incubated with anti-FLAG M2 Affinity Gel beads (Sigma-Aldrich) for 2 hrs at 4°C. The beads were washed 3 times with immunoprecipitation (IP) buffer (150 mM, NaCl, 50 mM Tris, pH 8, 1% NP-40, 0.25% sodium deoxycholate) and bound proteins were eluted by boiling in nondenaturing sample loading buffer and loaded onto PAGE gels. For detecting binding of Lef1 and Smad4, expression constructs for LEF1-HA were transiently transfected into HCT116 3:6 cells (stably expressing Smad4) for 48 hrs. Cells were then collected, lysed and immunoprecipitation was performed as described above followed by detection through western blot.

mRNA analysis.

RNA was extracted using the RNeasy Kit (Qiagen) and TRIzol (Invitrogen) and cDNA synthesis was performed using the Maxima First-Strand cDNA Synthesis kit (ThermoFisher). Quantitative PCR analysis using SYBRGreen PCR Master Mix (ThermoFisher) was performed according to standard procedures.

Scratch assay.

Confluent monolayers of cells were treated with 10 µg/ml of Mitomycin C (Sigma-Aldrich) for 3 hrs to stop cell proliferation and then wounded by scrapping the cells with a 200 µl pipette tip. Cells were then incubated in serum free medium with condition medium from Wnt3A-producing L cells or control L cells for 24hrs. Cells were photographed at 0hrs and 24hrs. The cell-free area (wound) area was measured using ImageJ software and the percentage of original wound area filled with cells was calculated. At least 3 independents series of experiments were performed.

RNA-seq.

Total RNA was extracted from SW480 cells using RNeasy Mini Kit (QIAGEN, #74104) and polyA+ transcripts were isolated with NEB Next Poly(A) mRNA Magnetic Isolation Module (NEB, #7490). RNA-Seq libraries were prepared with NEBNext Ultra II Directional RNA Library Prep Kit for Illumina (NEB, E7760S). Three biological replicates were sequenced on a NextSeq 500 (Illumina) at a depth of at least 2×10^7 reads each. Reads were mapped and analyzed with a bioinformatic pipeline based on GSNAP, featureCounts, and the R packages limma and edgeR. We used human genome version GRCh38. GO analyses were performed using version 6.8 of the DAVID web server. GSEA analyses were performed using pre-ranked GSEA using a weighted scoring.

Statistics and reproducibility.

All statistical analyses were carried out using Graph Pad Prism (version 7) by unpaired student's t-test for two group comparisons, Yate's continuity corrected chi-square test for contingency table analysis and Gehan-Breslow-Wilcoxon test for survival curves. Error bars represent s.e.m. \pm SD, and statistical significance was defined as $P < 0.05$.

RESULTS

SMAD4 R361 missense mutations prevalent in colorectal cancer result in loss of binding to phospho-Smad2/3.

To understand the clinical relevance of SMAD4 mutations in CRC, we analyzed *SMAD4* mutation data in the recent Memorial Sloan Kettering Cancer Center (MSKCC) study, which compiled cancer gene panel data corresponding to 1,134 colorectal adenocarcinomas from patients with both metastatic and early-stage CRC. While all TGF β signaling components were affected by some genetic alterations, *SMAD4* was the most frequently altered gene from the TGF β signaling pathway (22). Of all SMAD4 mutations and copy number alterations, missense mutations classified as putative drivers were the most abundant. Although they could be found across the MH2 domain, we confined subsequent analyses to amino acid substitutions in the R361 residue, as they were found at a much higher frequency than other missense mutations in this data set and other CRC studies (11,23) (Figure 1A).

To study the effects of R361 mutations in CRC cells, we generated retroviral constructs expressing either Smad4 wild-type (WT) or point mutations at the MH2 domain of Smad4, specifically at the arginine 361 residue (R361) and bearing FLAG tag at the N-terminus. We transduced those constructs into cell lines that lack detectable endogenous Smad4 protein, SW480 and SW620 (24), but have otherwise intact TGF β signaling pathway components (25) (Figure 1B). After transduction with the retroviral constructs, we were able to detect robust protein expression by Western blotting using the α -Smad4 antibody (Figure 1C). The effects of R361-mutations on Smad4 turnover were examined using cyclohexamide treatment (25 μ g/mL for 0, 6 and 12 hrs). We observed that both Smad4-WT and Smad4-R361H/C protein were turned over with similar kinetics (Figure 1D), suggesting that mutations at the R361 residue did not affect the half-life of Smad4 protein. To study the Smad4 mutations in additional TGF β -responsive cell lines, we used an HCT116 engineered derivative HCT116 3:6, in which TGF β signaling and the mismatch repair system were restored via human chromosome 3 transfer (26). To render them Smad4-deficient, we used Santa Cruz CRISPR-Cas9 knockout (KO) and homology directed repair (HDR) plasmid according to manufacturer's protocol. Edited HCT116 3:6 cells were cloned using flow cytometry and a single cell clone with no trace of Smad4 expression was identified using Western blotting (Figure S1A). These cells were also transduced with SMAD4 retroviruses resulting in expression levels exceeding those seen in parental HCT116 3:6 cells by no more than 3-fold (Figure S1B). Thus, although levels of retrovirally expressed Smad4 did not exactly match those seen in CRC, they were not grossly elevated either.

Because Smad4 is an important factor in TGF β signaling, we asked whether there were major differences in R-Smad phosphorylation between wild type- and R361H/C-mutant cells. Stimulation of SW480 and SW620 cell lines for 1 hour with 5 ng/mL of TGF β resulted in phosphorylation of both R-Smads regardless of Smad4 status (Figure 1E). This was not surprising, given that TGF β -induced phosphorylation of Smad2/3 occur upstream of Smad4. However, R361 maps to the loop-helix region of the Smad4 MH2 domain and is an important residue in forming Smad4 heterocomplexes with R-Smads (27). To test whether mutations at the R361 residue were able to bind to phosphorylated Smad2 and Smad3, we

performed immunoprecipitation analysis on SW480 and HCT116 3:6 CRC cells treated with either vehicle control or soluble TGF β . While wild-type Smad4 was able to bind to both R-Smads, both R361H and R361C mutations completely abolished interaction with R-Smads (Figure 1F and S1C). These findings suggested that R361 missense mutations do not affect overall phosphorylation of Smad2/3, they effectively abolish heterodimerization between Smad4 and pSmad2/3.

Smad4 mutants do not support canonical TGF β -induced transcriptional activity.

Activated Smad2/3/4 complexes accumulate in the nucleus, where they can bind directly or indirectly to DNA and regulate gene expression. Because Smad4 is a critical effector of TGF β signaling, we tested whether R361 mutations in Smad4 alter its transcriptional activity. To this end, Smad4 wild-type and R361H/C mutant-expressing cell lines were transiently transfected with the SBE4-luc vector containing 4 copies of the Smad binding element (SBE), a sequence that allows for strong Smad-DNA binding (28). A weaker p3TP-Lux reporter was previously shown to be unresponsive to TGF β in Smad4-reconstituted SW480 cells (29). As expected, Smad4-WT was able to support downstream TGF β transcriptional activity in the presence of soluble TGF β in all three of our CRC cell lines (SW480, SW620 and HCT116 3:6). However, both Smad4 R361 mutations were unable to support canonical TGF β transcriptional activity and behaved similarly to the empty vector-transduced cells (Figure 2A and S1D). There has been uncertainty as to whether mutations in Smad4 could exert a dominant-negative effect over Smad4-WT (30,31). We therefore tested the ability of mutant Smad4 to interfere with Smad4-mediated TGF β -responsive transcription. Due to ease of transfection, we used the HCT116 3:6 Smad4 knockout (KO) clone from panel S1A and observed that transfecting increasing amounts of either Smad4-R361H or -R361C had no effect on induction of SBE reporter activity by TGF β (Figure S1E) arguing against the dominant negative mechanism.

To further confirm the decrease in transcriptional activity of Smad4-R361 mutants, we performed quantitative analysis of Smad4-targeted gene expression by real-time quantitative RT-PCR (qRT-PCR). The expression of *PAI-1* and *SNAI2*, both well-validated direct Smad4 target genes, was compared in SW480 and HCT116 3:6 cells expressing different Smad4 constructs or the empty vector. Consistent with the reporter assay, in both SW480 and HCT116 3:6 TGF β -treated cells, only Smad4-WT was able to induce the expression of these Smad4 target genes by more than 2-fold, whereas this induction was not seen in cells expressing Smad4 R361 mutants (Figure 2B and S1F). Furthermore, since Smad4 binds directly to the well-characterized promoter region of PAI-1 (32), we performed chromatin immunoprecipitation (ChIP) assay followed by qPCR. As expected, stimulation of SW480 cells with TGF β induced the recruitment of Smad4-WT, but not Smad4 R361 mutant proteins to the promoter region of PAI-1 (Figure 2C). Taken together, these data indicated that Smad4-R361 mutations completely disengage from the TGF β pathway and neither activate nor repress canonical TGF β signaling.

R361H confers the gene signature associated with Lef1 protein overexpression.

Although with respect to canonical TGF β targets Smad4-R361 mutations act in a loss-of-function manner, we reasoned that a hotspot mutation is more consistent with a gain-of-

function mechanism. To uncover such a mechanism, we performed RNA-Seq analysis on SMAD4-transduced SW480 cells treated with soluble TGF β for 24 hr. Principal component analysis (PCA) performed on all expression datasets revealed that as expected, Smad4-WT was the only group strongly affected by the treatment with soluble TGF β (Figure 3A). However, unexpectedly, the SMAD4 mutant samples separated very strongly from the SMAD4-null samples, with or without TGF β treatment. This separation was the first experimental evidence of non-equivalence of SMAD4-null and missense mutations. To understand the specific differences between CRC cells expressing no Smad4 vs Smad4 R361 mutants, we further analyzed our RNA-Seq data set by gene set enrichment analysis (GSEA) (33). We discovered that Smad4-R361H-associated genes are most significantly enriched in the members of the following datasets: genes down or up-regulated in DLD1 cells (colon carcinoma) over-expressing Lef1 (Figure 3B). This enrichment was strongly driven by the cluster of genes that were expressed at high levels in SMAD4-null cell but downregulated in SMAD4-WT and especially in SMAD4-MUT cells (Figure 3C) such as known colon cancer metastasis suppressor PRSS8 (34), putative CRC tumor suppressor RAB25 (35), and an NF- κ B inhibitor NLRP2 (36). To confirm that a transcriptome associated with Lef1-levels was indeed affected, we confirmed the RNA-seq results by analyzing single genes by qRT-PCR. Indeed, we saw that mRNA expression of all three genes of interest (*PRSS8*, *RAB25*, *NLRP2*) was downregulated in cells expressing Smad4 R361H and R361C mutants compared to empty vector-transduced cells, with only RAB25 transcript in R361H cells failing to reach statistical significance (Figure 3D). Essentially identical results were obtained using HCT116 3:6 cells (Figure S2A), suggesting that dysregulation of Lef1 targets in SMAD4 R361 mutant CRC cells is a generalizable effect.

To study this effect at the molecular level, we first measured the levels of Lef1 protein in empty vector, Smad4-WT and Smad4-R361 CRC cells and observed no different in expression levels (Figure 4A). Previous studies have demonstrated that Smad4-WT and Lef1 can bind each other in neuroblastoma and fibroblast-like cells (37,38). To investigate whether or not Smad4-R361 mutants can bind Lef1 protein in cells of epithelial origin, including CRC cells, we transiently co-transfected FLAG-tagged Smad4 constructs and HA-tagged LEF1 construct into HEK cells. In parallel, we transfected HA-tagged LEF1 into Smad4-transduced HCT116 3:6 cultures with HA-LEF1. Then, we performed immunoprecipitation with an anti-FLAG antibody followed by immunoblotting for HA. In both cases we observed that Smad4-WT as well as Smad4-R361H/C can bind Lef1 (Figures S2B and 4B, respectively), but the importance of this interaction for cancer cell biology remained to be determined.

As Lef1 is a key downstream effector of the Wnt pathway, we evaluated Wnt signaling status in our CRC cell lines. Specifically, we employed the TOP-Flash/FOP-Flash luciferase reporter that contains 7 copies of TCF/LEF binding sites. Even when incubated in basal media, R361 Smad4 mutants were able to boost Wnt signaling to higher levels compared to no-Smad4 and wild-type Smad4 in both SW480 and HCT116 3:6 cells (Figure S2C). Since SW480 are not responsive to exogenous Wnt3a, we continued our studies with HCT116 3:6 cells. When HCT116 3:6 Smad4 cells were treated with soluble Wnt3a ligand, we observe an increase in Wnt signaling compared to vehicle control. In addition, there was robust and highly significant up-regulation of Wnt signaling by R361 mutants when compared to cells

expressing both no-Smad4 and even wild-type Smad4 (Figure 4C). Yet the importance of Smad4-Lef1 interaction for this up-regulation remained to be determined.

It has been previously shown amino acids 511–552 are crucial for interaction of SMAD4 with Lef1 (38). Thus, we have generated a series of nested Smad4 deletions covering that region. Then they were co-transfected, along with the HA-tagged LEF1 construct, into Smad4-transduced HCT116 3:6 cultures, and co-immunoprecipitation/immunoblotting analyses were carried out. We observed that even a smaller Smad4 aa543–535 deletion reduced Lef1 binding to background levels (Figure 4D). To determine if this loss of Smad4-Lef1 interaction negatively impacts Wnt signaling, we once again used the TOP/FOP reporter assay. While Smad4-WT, R361H and R361C upregulated Wnt signaling as expected, Smad4 aa543–535 behaved no differently from the empty vector (Figure 4E). To extend this finding to important cancer phenotypes, we performed in vitro scratch assay, which measures the ability of motile cancer cells to close gaps in 2D-monolayers. The experiments were performed in serum-free media conditioned by either Wnt3A-producing or parental L cells for 24 hrs; the “wound” closure under Wnt3a vs control conditions was reflective of the strength of Wnt signaling. The results were fully consistent with the TOP/FOP assay, in that both R361 mutants promoted Wnt signaling more strongly than wild type protein and the aa543–552 mutant (Figure 4F and G). Collectively, these results suggested that Smad4 amino acids 543–552 are essential for binding to Lef1, and by inference that Smad4-Lef1 binding is essential for Wnt upregulation.

Wnt activation and SMAD4 missense mutations in primary CRCs.

We then asked whether there is an epistatic relationship between Smad4 missense mutations and Wnt activation in CRC patients. To answer this question, we re-analyzed the MSKCC cancer panel study. In microsatellite stable CRC samples, *SMAD4* has a 15% frequency of mutation while *CTNNB1* (β -catenin) has a lower mutation frequency of 4% (Figure 5A), likely due to *APC* already being mutated in many CRC patients (39). We reasoned that if *SMAD4* missense mutations aid Wnt signaling, activating missense mutation in *CTNNB1* will be under even less selective pressure to occur. This would be in contrast to *SMAD4* truncating mutations, which do not affect Wnt signaling. To compare and contrast the co-occurrence frequency of *CTNNB1* mutations in CRCs alongside either *SMAD4* missense or loss-of-function nonsense mutations (31,40), we utilized the chi-square test with Yate’s correction. Indeed, we observed highly statistically significant enrichment for *CTNNB1* mutations in CRC with nonsense mutations, at the expense of tumors with *SMAD4* missense mutations (Figure 5B).

Finally, to understand the contribution of R361-mutations to clinical outcomes in CRC patients, we analyzed median overall survival (OS) in the MSKCC cohort. When compared with patients with no *SMAD4* alterations, patients with *SMAD4* missense mutations had a shorter OS survival of 70.03 vs 40.5 months ($p = 0.0186$). This difference was not observed in patients that had no alteration for *SMAD4* versus patients with *SMAD4* truncating nonsense mutations (OS survival of 70.03 vs 68.3 months respectively, $p = 0.9076$) (Figure 5C, left and right). These data demonstrate that CRC patients with *SMAD4*

missense mutations do worse overall than those with unaltered SMAD4 and truncating mutations in SMAD4, attesting to gain-of-function properties of the former.

DISCUSSION

Defects in Smad4 play a significant role in the malignant progression of tumors and are frequently altered in colon and pancreatic carcinomas (7,22). About 10–30% of CRC patients harbor some loss of Smad4, either by deep deletion or nonsense mutations. Interestingly, missense mutations in Smad4 also have been identified in variety of cancers including CRC. In these tumors, Smad4 mutations appear frequently at the MH2 domain. By analyzing both primary tumors and immortalized cells lines, two of the most frequent Smad4 missense mutations have been identified at position 361 which results in a substitution from arginine to either histidine or cysteine (16) These genetic hits are recurrently detected in the Smad4 locus, consistent with the idea that this gene acts as a tumor suppressor. On the other hand, their clustering in distinct hot spots argues that Smad4 mutants, similar to mutant TP53 (41), might have an oncogenic function; however this hypothesis has not been previously tested.

In the present study, we investigated the functional roles of the missense mutations R361H and R361C in the Smad4 MH2 domain that naturally occur in human colorectal cancer patients (16). This was achieved by the means of retroviral transduction into cell lines that lack endogenous Smad4 protein. Smad4 missense mutations had been previously mapped onto the crystal structures of Smad heterodimers, specifically onto the defined protein loop that is directly involved in binding to the R-Smads. Our co-immunoprecipitation experiments indicate that point mutations in Smad4 MH2 domain indeed disrupt binding to endogenous p-Smad2 or p-Smad3. We also showed in transfection assays that Smad4 missense mutations cannot support transcription from reporters driven by Smad3–Smad4 (CAGA12-luciferase) complexes. Admittedly, some tumor suppressor genes can have dominant negative effects. For example, mutant p53 protein can bind to its wild type counterpart encoded by the unaltered allele and sequester it in non-functional complexes (42). However, when we co-expressed mutant and wild-type Smad4, we observed no dominant negative effects of the former. Taken at face value, these experiments would suggest that Smad4 variants are loss-of-function. This mechanism is supported by several lines of genetic evidence, including a frequent loss of heterozygosity (LOH) at chromosome locus 18q where SMAD4 is located; such loss is associated with a poor prognosis for CRC patients (43,44). Yet the very high prevalence of R361 SMAD4 mutations in CRC patients, particularly in those with distant metastasis vs. locally advanced tumors (35% vs. 10% respectively) (45) indicated that additional molecular mechanisms could be at play.

Here, using the RNA-seq approach and Gene Set Enrichment Analysis, we demonstrate that Smad4 R361mut cells acquire the known gene signature associated with enhanced Lef1 protein function and increased Wnt signaling. In search of the underlying mechanism, we discovered that Smad4 mutant proteins, while defective in R-Smad binding, retain the previously reported affinity of the wild type protein for Lef1 (37,38,46). Consistent with this biochemical property, they drive a commensurate increase in downstream Wnt signaling as measured by TOP/FOP luciferase assay and Wnt-dependent cell motility. Of note, a 10-

amino acid deletion in Smad4 (aa543–552) abolishes both Lef1 binding and Wnt activation, suggesting that the Smad4-Lef1 interaction plays a key role in sustaining robust Wnt signaling.

Admittedly, our results are at variance with the report by Freeman et al claiming that restoration of Smad4 in CRC cells can lead to suppression of Wnt signaling via repression of β -catenin expression (47). There are several possible reasons for the discrepancy between our results, chief among them the differences in the experimental setups. For example, Freeman and co-authors employed transient transfection of Smad4 constructs, which typically yields much higher protein levels than retroviral transduction. Of note, in our RNA-seq experiments we did not observe dysregulation of the beta-catenin mRNA, suggesting that regulation of the CTNNB1 transcription by Smad4 could be dose-dependent. Furthermore, in Freeman et al the effects of Smad4 on CTNNB1 transcription were at least partly realized through BMP signaling, which was not under investigation in our study. Finally, as a readout for Wnt activity Freeman et al relied exclusively on the TOP-flash reporter, whereas we utilized the internally controlled TOP-FOP dual plasmid system (48). We also used additional readouts such as transcriptome profiling combined with Gene Set Enrichment Analysis (GSEA). All this makes direct comparison somewhat difficult, but also underscores the complex nature of Smad4 effects.

Moreover, it didn't escape our attention that there is more Wnt signaling in Smad4-R361 CRC expressing cells compared to those expressing Smad4-WT. It is possible that the inability of Smad4 R361 mutant to bind R-Smads following TGF β stimulation increases the pool of available protein to bind to Lef1; however, more experimentation will be required to test this hypothesis. In addition, it is possible that the unique Lef1-Smad-R361 complex specifically recruits other transcription factors, such as β -catenin, to assist in downstream activation of Wnt signaling. However, Smad4- β -catenin binding has been understudied and independent publications yielded mixed results (49–51). The underlying molecular mechanism notwithstanding, human CRCs with SMAD4 missense mutations are less likely to acquire activating mutations in the key Wnt pathway gene CTNNB1 (which encodes β -catenin) than CRCs with truncating SMAD4 nonsense mutations. How this TGF β -independent gain of function by mutant Smad4 shapes the CRC biology likely depends on cooperating genetic and possibly epigenetic events.

At least two major genomic pathways are involved in the initiation and progression of CRC: microsatellite instability (MSI) and chromosomal instability (CIN) (52). Six research groups identified a consensus for gene expression based on a subtyping classification system for CRC, which resulted in four consensus molecular subtypes (CMS) (53). The four subtypes differ in genetic and epigenetics, as well as the signaling pathways they follow. While CMS1 is characteristic of tumors with MSI, tumors with CIN can be subclassified on the basis of gene expression: CMS2 (canonical subtype), CMS3 (metabolic subtype) and CMS4 (mesenchymal subtype) (54). Copy number variation in both oncogenes and tumor suppressor genes are found more frequently in CMS2 than in other subtypes and they display a strong upregulation of Wnt and MYC downstream targets. Interestingly, SMAD4 mutations were profiled across different molecular subtypes and found to be most common with the CMS3 subtype (11), however that classification was not specific to SMAD4

missense mutations. Based on our data and the overall working model, we would expect that SMAD4 missense mutation (especially hotspot mutation R361) is commonly found in the CMS2 subtype due to their marked upregulation of Wnt pathway. However, this hypothesis could not be tested directly using our dataset due to the lack of RNA-Seq data in the MSKCC cohort (22). It also precluded us from comparing WNT signatures in the presence and absence of missense mutations in SMAD4. Nevertheless, based on our survival analysis, the interaction between Smad4-R361 and LEF/TCF protein complexes may shape therapeutic responses, including but not limited to heightened sensitivity to Wnt pathway inhibitors.

In support of this notion, loss of Smad4 has been shown to induce tumorigenicity and 5-FU (5-fluoracil) resistance through activation of the Akt pathway, which results in upregulation of anti-apoptotic proteins (55). Another study revealed that patients with advanced disease observed a markedly shorter progression-free survival time in patients with *SMAD4*-mutated tumors than in those wild-type for *SMAD4*, when treated with epidermal growth factor receptor (EGFR) inhibitors (11). This suggests that mutant Smad4 might be affecting signaling pathways other than TGF β and Wnt, possibly via binding to other, yet to be identified transcription factors.

Supplementary Material

Refer to Web version on PubMed Central for supplementary material.

ACKNOWLEDGEMENTS

We thank all the members of our laboratories and that of Dr. Roger Gomis (IRB Barcelona) for many helpful discussions. Dr. Lanauze gratefully acknowledges the members of her thesis committee: Drs. Christopher Lengner, Ellen Pure (University of Pennsylvania), Brian Keith (Wistar Institute), and Anil Rustgi (Columbia University).

Financial Support

This work was supported by NIH grants R01 CA196299 (ATT) and 5T32 CA009140 (CL). SFAG is supported by the Daniel B. Burke Endowed Chair for Diabetes Research.

REFERENCES

1. Massagué J TGF β signalling in context. *Nat Rev Mol Cell Biol* 2012;13(10):616–30. [PubMed: 22992590]
2. Derynck R, Zhang YE. Smad-dependent and Smad-independent pathways in TGF-beta family signalling. *Nature* 2003;425(6958):577–84. [PubMed: 14534577]
3. Seoane J, Gomis RR. TGF-beta family signaling in tumor suppression and cancer progression. *Cold Spring Harb Perspect Biol* 2017;9(12).
4. Fearon ER. Molecular genetics of colorectal cancer. *Annu Rev Pathol* 2011;6:479–507. [PubMed: 21090969]
5. Zhao M, Mishra L, Deng CX. The role of TGF-beta/SMAD4 signaling in cancer. *Int J Biol Sci* 2018;14(2):111–23. [PubMed: 29483830]
6. Muzny DM, Bainbridge MN, Chang K, Dinh HH, Drummond JA, Fowler G, et al. Comprehensive molecular characterization of human colon and rectal cancer. *Nature* 2012;487(7407):330–7. [PubMed: 22810696]
7. Alazzouzi H, Alhopuro P, Salovaara R, Sammalkorpi H, Jarvinen H, Mecklin JP, et al. SMAD4 as a prognostic marker in colorectal cancer. *Clin Cancer Res* 2005;11(7):2606–11. [PubMed: 15814640]

8. Papageorgis P, Cheng K, Ozturk S, Gong Y, Lambert AW, Abdolmaleky HM, et al. Smad4 inactivation promotes malignancy and drug resistance of colon cancer. *Cancer Res* 2011;71(3):998–1008. [PubMed: 21245094]
9. Iacobuzio-Donahue CA, Song J, Parmigiani G, Yeo CJ, Hruban RH, Kern SE. Missense mutations of MADH4: characterization of the mutational hot spot and functional consequences in human tumors. *Clin Cancer Res* 2004;10(5):1597–604. [PubMed: 15014009]
10. Woodford-Richens KL, Rowan AJ, Poulson R, Bevan S, Salovaara R, Aaltonen LA, et al. Comprehensive analysis of SMAD4 mutations and protein expression in juvenile polyposis: evidence for a distinct genetic pathway and polyp morphology in SMAD4 mutation carriers. *Am J Pathol* 2001;159(4):1293–300. [PubMed: 11583957]
11. Mehrvarz Sarshekeh A, Advani S, Overman MJ, Manyam G, Kee BK, Fogelman DR, et al. Association of SMAD4 mutation with patient demographics, tumor characteristics, and clinical outcomes in colorectal cancer. *PLoS One* 2017;12(3):e0173345. [PubMed: 28267766]
12. Kim E, Ilic N, Shrestha Y, Zou L, Kamburov A, Zhu C, et al. Systematic Functional Interrogation of Rare Cancer Variants Identifies Oncogenic Alleles. *Cancer Discov* 2016;6(7):714–26. [PubMed: 27147599]
13. Dews M, Tan GS, Hultine S, Raman P, Choi J, Duperret EK, et al. Masking epistasis between MYC and TGF-beta pathways in antiangiogenesis-mediated colon cancer suppression. *J Natl Cancer Inst* 2014;106(4):dju043. [PubMed: 24627270]
14. Schwarte-Waldhoff I, Volpert OV, Bouck NP, Sipos B, Hahn SA, Klein-Scory S, et al. Smad4/DPC4-mediated tumor suppression through suppression of angiogenesis. *Proc Natl Acad Sci USA* 2000;97(17):9624–9. [PubMed: 10944227]
15. Losi L, Bouzourene H, Benhattar J. Loss of Smad4 expression predicts liver metastasis in human colorectal cancer. *Oncol Rep* 2007;17(5):1095–9. [PubMed: 17390050]
16. Fleming NI, Jorissen RN, Mouradov D, Christie M, Sakthianandeswaren A, Palmieri M, et al. SMAD2, SMAD3 and SMAD4 mutations in colorectal cancer. *Cancer Res* 2013;73(2):725–35. [PubMed: 23139211]
17. Shi Y, Hata A, Lo RS, Massague J, Pavletich NP. A structural basis for mutational inactivation of the tumour suppressor Smad4. *Nature* 1997;388(6637):87–93. [PubMed: 9214508]
18. Pierreux CE, Nicolas FJ, Hill CS. Transforming growth factor beta-independent shuttling of Smad4 between the cytoplasm and nucleus. *Mol Cell Biol* 2000;20(23):9041–54. [PubMed: 11074002]
19. Moren A, Hellman U, Inada Y, Imamura T, Heldin CH, Moustakas A. Differential ubiquitination defines the functional status of the tumor suppressor Smad4. *J Biol Chem* 2003;278(35):33571–82. [PubMed: 12794086]
20. Zhan T, Rindtorff N, Boutros M. Wnt signaling in cancer. *Oncogene* 2017;36(11):1461–73. [PubMed: 27617575]
21. Sakai S, Ohhata T, Kitagawa K, Uchida C, Aoshima T, Niida H, et al. Long Noncoding RNA ELIT-1 Acts as a Smad3 Cofactor to Facilitate TGFβ/Smad Signaling and Promote Epithelial-Mesenchymal Transition. *Cancer Res* 2019;79(11):2821–38. [PubMed: 30952633]
22. Yaeger R, Chatila WK, Lipsyc MD, Hechtman JF, Cercek A, Sanchez-Vega F, et al. Clinical sequencing defines the genomic landscape of metastatic colorectal cancer. *Cancer Cell* 2018;33(1):125–36 e3. [PubMed: 29316426]
23. Brannon AR, Vakiani E, Sylvester BE, Scott SN, McDermott G, Shah RH, et al. Comparative sequencing analysis reveals high genomic concordance between matched primary and metastatic colorectal cancer lesions. *Genome Biol* 2014;15(8):454. [PubMed: 25164765]
24. Woodford-Richens KL, Rowan AJ, Gorman P, Halford S, Bicknell DC, Wasan HS, et al. SMAD4 mutations in colorectal cancer probably occur before chromosomal instability, but after divergence of the microsatellite instability pathway. *Proc Natl Acad Sci USA* 2001;98(17):9719–23. [PubMed: 11481457]
25. Ahmed D, Eide PW, Eilertsen IA, Danielsen SA, Eknaes M, Hektoen M, et al. Epigenetic and genetic features of 24 colon cancer cell lines. *Oncogenesis* 2013;2(0424):e71. [PubMed: 24042735]
26. Koi M, Umar A, Chauhan DP, Cherian SP, Carethers JM, Kunkel TA, et al. Human chromosome 3 corrects mismatch repair deficiency and microsatellite instability and reduces N-methyl-N'-nitro-

- N-nitrosoguanidine tolerance in colon tumor cells with homozygous hMLH1 mutation. *Cancer Res* 1994;54(16):4308–12. [PubMed: 8044777]
27. Shi Y, Massagué J. Mechanisms of TGF- β signaling from cell membrane to the nucleus. *Cell* 2003;113(6):685–700. [PubMed: 12809600]
 28. Zawel L, Dai LJ, Buckhaults P, Zhou S, Kinzler KW, Vogelstein B, et al. Human Smad3 and Smad4 are sequence-specific transcription activators. *Mol Cell* 1998;1(4):611–7. [PubMed: 9660945]
 29. Shiou SR, Singh AB, Moorthy K, Datta PK, Washington MK, Beauchamp RD, et al. Smad4 regulates claudin-1 expression in a transforming growth factor-beta-independent manner in colon cancer cells. *Cancer Res* 2007;67(4):1571–9. [PubMed: 17308096]
 30. Pardali K, Kurisaki A, Moren A, ten Dijke P, Kardassis D, Moustakas A. Role of Smad proteins and transcription factor Sp1 in p21(Waf1/Cip1) regulation by transforming growth factor-beta. *J Biol Chem* 2000;275(38):29244–56. [PubMed: 10878024]
 31. Maurice D, Pierreux CE, Howell M, Wilentz RE, Owen MJ, Hill CS. Loss of Smad4 function in pancreatic tumors: C-terminal truncation leads to decreased stability. *J Biol Chem* 2001;276(46):43175–81. [PubMed: 11553622]
 32. Dennler S, Itoh S, Vivien D, ten Dijke P, Huet S, Gauthier JM. Direct binding of Smad3 and Smad4 to critical TGF beta-inducible elements in the promoter of human plasminogen activator inhibitor-type 1 gene. *EMBO J* 1998;17(11):3091–100. [PubMed: 9606191]
 33. Subramanian A, Tamayo P, Mootha VK, Mukherjee S, Ebert BL, Gillette MA, et al. Gene set enrichment analysis: a knowledge-based approach for interpreting genome-wide expression profiles. *Proc Natl Acad Sci USA* 2005;102(43):15545–50. [PubMed: 16199517]
 34. Bao Y, Guo Y, Yang Y, Wei X, Zhang S, Zhang Y, et al. PRSS8 suppresses colorectal carcinogenesis and metastasis. *Oncogene* 2019;38(4):497–517. [PubMed: 30115975]
 35. Goldenring JR, Nam KT. Rab25 as a tumour suppressor in colon carcinogenesis. *Br J Cancer* 2011;104(1):33–6. [PubMed: 21063400]
 36. Liu S, Fan W, Gao X, Huang K, Ding C, Ma G, et al. Estrogen receptor alpha regulates the Wnt/beta-catenin signaling pathway in colon cancer by targeting the NOD-like receptors. *Cell Signal* 2019;61(April):86–92. [PubMed: 31121307]
 37. Labbe E, Letamendia A, Attisano L. Association of Smads with lymphoid enhancer binding factor 1/T cell-specific factor mediates cooperative signaling by the transforming growth factor-beta and wnt pathways. *Proc Natl Acad Sci USA* 2000;97(15):8358–63. [PubMed: 10890911]
 38. Qu H, Zheng L, Jiao W, Mei H, Li D, Song H, et al. Smad4 suppresses the tumorigenesis and aggressiveness of neuroblastoma through repressing the expression of heparanase. *Sci Rep* 2016;6(February):32628. [PubMed: 27595937]
 39. Schneikert J, Behrens J. The canonical Wnt signalling pathway and its APC partner in colon cancer development. *Gut* 2007;56(3):417–25. [PubMed: 16840506]
 40. Yoshioka Y, Togashi Y, Chikugo T, Kogita A, Taguri M, Terashima M, et al. Clinicopathological and genetic differences between low-grade and high-grade colorectal mucinous adenocarcinomas. *Cancer* 2015;121(24):4359–68. [PubMed: 26488212]
 41. Willis A, Jung EJ, Wakefield T, Chen X. Mutant p53 exerts a dominant negative effect by preventing wild-type p53 from binding to the promoter of its target genes. *Oncogene* 2004;23(13):2330–8. [PubMed: 14743206]
 42. Payne SR, Kemp CJ. Tumor suppressor genetics. *Carcinogenesis* 2005;26(12):2031–45. [PubMed: 16150895]
 43. Arai T, Akiyama Y, Yamamura A, Hosoi T, Shibata T, Saitoh K, et al. Allelotype analysis of early colorectal cancers with lymph node metastasis. *Int J Cancer* 1998;79(4):418–23. [PubMed: 9699536]
 44. Martinez-Lopez E, Abad A, Font A, Monzo M, Ojanguren I, Pifarre A, et al. Allelic loss on chromosome 18q as a prognostic marker in stage II colorectal cancer. *Gastroenterology* 1998;114(6):1180–7. [PubMed: 9609754]
 45. Miyaki M, Iijima T, Konishi M, Sakai K, Ishii A, Yasuno M, et al. Higher frequency of Smad4 gene mutation in human colorectal cancer with distant metastasis. *Oncogene* 1999;18(20):3098–103. [PubMed: 10340381]

46. Lim SK, Hoffmann FM. Smad4 cooperates with lymphoid enhancer-binding factor 1/T cell-specific factor to increase c-myc expression in the absence of TGF-beta signaling. *Proc Natl Acad Sci USA* 2006;103(49):18580–5. [PubMed: 17132729]
47. Freeman TJ, Smith JJ, Chen X, Washington MK, Roland JT, Means AL, et al. Smad4-mediated signaling inhibits intestinal neoplasia by inhibiting expression of β -catenin. *Gastroenterology* 2012;142(3):562–71.e2. [PubMed: 22115830]
48. Veeman MT, Slusarski DC, Kaykas A, Louie SH, Moon RT. Zebrafish prickle, a modulator of noncanonical Wnt/Fz signaling, regulates gastrulation movements. *Curr Biol* 2003;13(8):680–5. [PubMed: 12699626]
49. Tian X, Zhang J, Tan TK, Lyons JG, Zhao H, Niu B, et al. Association of beta-catenin with P-Smad3 but not LEF-1 dissociates in vitro profibrotic from anti-inflammatory effects of TGF-beta1. *J Cell Sci* 2013;126(Pt 1):67–76. [PubMed: 23203799]
50. Voorneveld PW, Kodach LL, Jacobs RJ, van Noesel CJ, Peppelenbosch MP, Korkmaz KS, et al. The BMP pathway either enhances or inhibits the Wnt pathway depending on the SMAD4 and p53 status in CRC. *Br J Cancer* 2015;112(1):122–30. [PubMed: 25393365]
51. Calvo-Sanchez MI, Fernandez-Martos S, Carrasco E, Moreno-Bueno G, Bernabeu C, Quintanilla M, et al. A role for the Tgf-beta/Bmp co-receptor Endoglin in the molecular oscillator that regulates the hair follicle cycle. *J Mol Cell Biol* 2019;11(1):39–52. [PubMed: 30239775]
52. Domenica F, Palma DE, Argenio VD, Pol J, Kroemer G, Maiuri MC, et al. The molecular hallmarks of the serrated pathway in colorectal cancer. *Cancers* 2019;11(1017):3–5.
53. Guinney J, Dienstmann R, Wang X, de Reynies A, Schlicker A, Soneson C, et al. The consensus molecular subtypes of colorectal cancer. *Nat Med* 2015;21(11):1350–6. [PubMed: 26457759]
54. Dienstmann R, Vermeulen L, Guinney J, Kopetz S, Tejpar S, Tabernero J. Consensus molecular subtypes and the evolution of precision medicine in colorectal cancer. *Nat Rev Cancer* 2017;17(2):79–92. [PubMed: 28050011]
55. Zhang B, Zhang B, Chen X, Bae S, Singh K, Washington MK, et al. Loss of Smad4 in colorectal cancer induces resistance to 5-fluorouracil through activating Akt pathway. *Br J Cancer* 2014;110(4):946–57. [PubMed: 24384683]

Implications:

Our studies suggest that in CRC hotspot mutations in Smad4 confer enhanced Wnt signaling and possibly heightened sensitivity to Wnt pathway inhibitors.

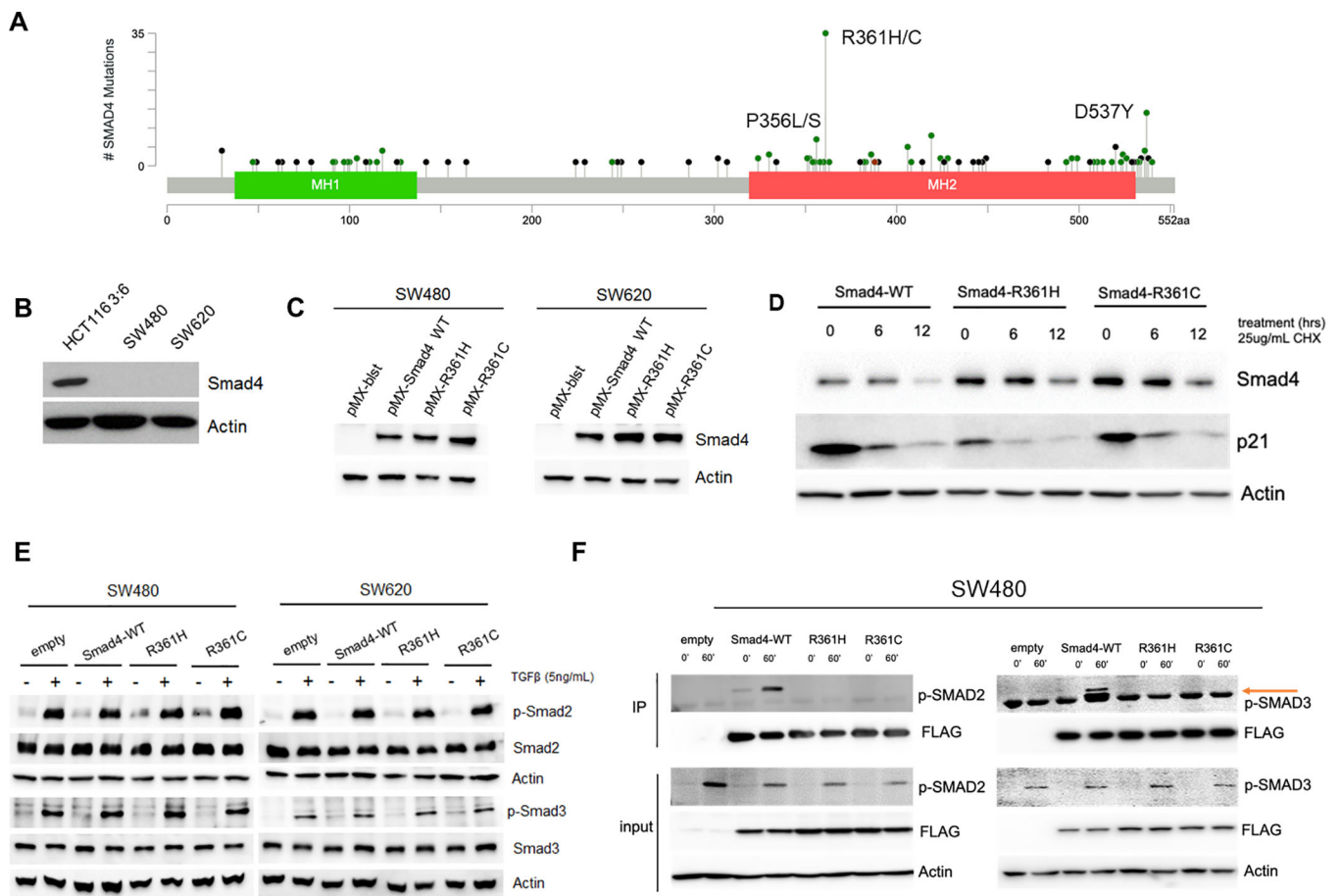


Figure 1. Smad4-R361 mutants do not bind to p-Smad2/3 in TGFβ-treated CRC cells.

(A) The prevalence and spectrum of SMAD4 mutations in MSKCC study. Black, green, and red “lollipops” represent nonsense and missense mutations and in-frame indels, respectively. Need to amend figure legend (B) Western blotting analysis of SW480/620 cell lines lacking endogenous expression of Smad4. HCT116 3:6 cells were used as the positive control. (C) Western blotting confirming ectopic expression of Smad4 in retrovirally transduced SW480 and SW620 cells. (D) Analysis of Smad4 expression by Western blotting in SW480 cells treated with 25ug/mL of cycloheximide for 0, 6 or 12 hrs. p21 was used as a labile control and actin was used as a loading control, here and in all subsequent Figures. (E) Analysis of R-Smad phosphorylation by Western blotting in SW480 and SW620 cells treated with either vehicle control or TGFβ (5 ng/mL) for one hour. Total levels of Smad2 and Smad3 were also measured as indicated. (F) Analysis of Smad4-R-Smad interactions in SW480 cells treated for 0' or 60' with soluble TGFβ. Co-immunoprecipitation was performed using FLAG-conjugated beads and Western blotting was subsequently performed using indicated antibodies. Whole cell lysates were used as an input control.

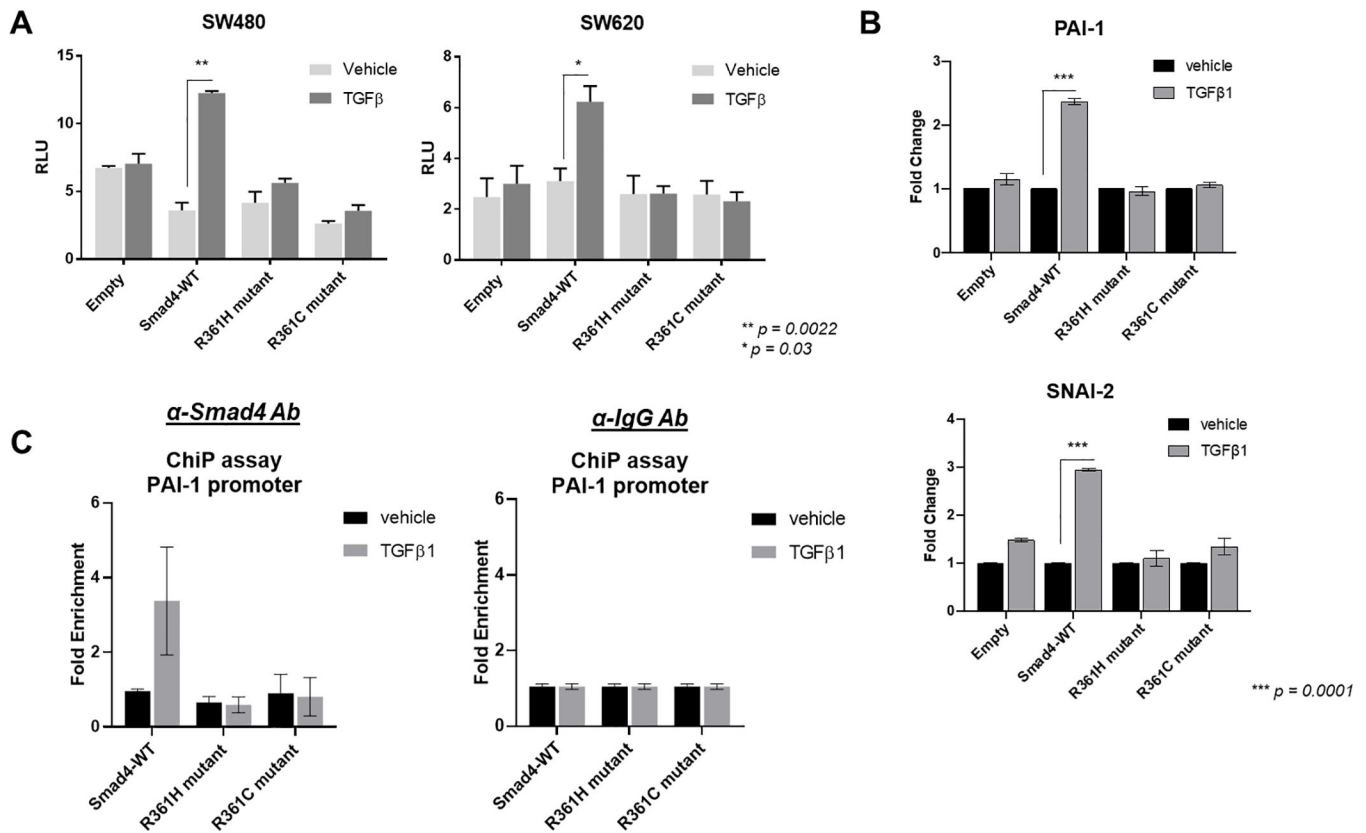


Figure 2. Stably expressed Smad4-R361 mutants do not support canonical TGFβ-induced transcriptional activity.

(A) Analysis of TGFβ signaling in SW480 and SW620 cells transfected with the SBE-Luciferase construct and subsequently treated with either vehicle control or soluble TGFβ ligand. pRL-TK plasmid was used as an internal control. (B) Induction of PAI-1 (top) and SNAI2 (bottom) transcripts by TGFβ in SW480 cells, as measured by qRT-PCR. (C) Binding of Smad4 to the PAI-1 promoter in SW480 cells, as measured by ChIP-qPCR. Cell cultures were pretreated with vehicle control or 10ng/mL of soluble TGFβ for one hour. Chromatin fraction from harvested cells were incubated with the anti-Smad4 antibody or control IgG. These experiments were performed twice, and representative data are shown.

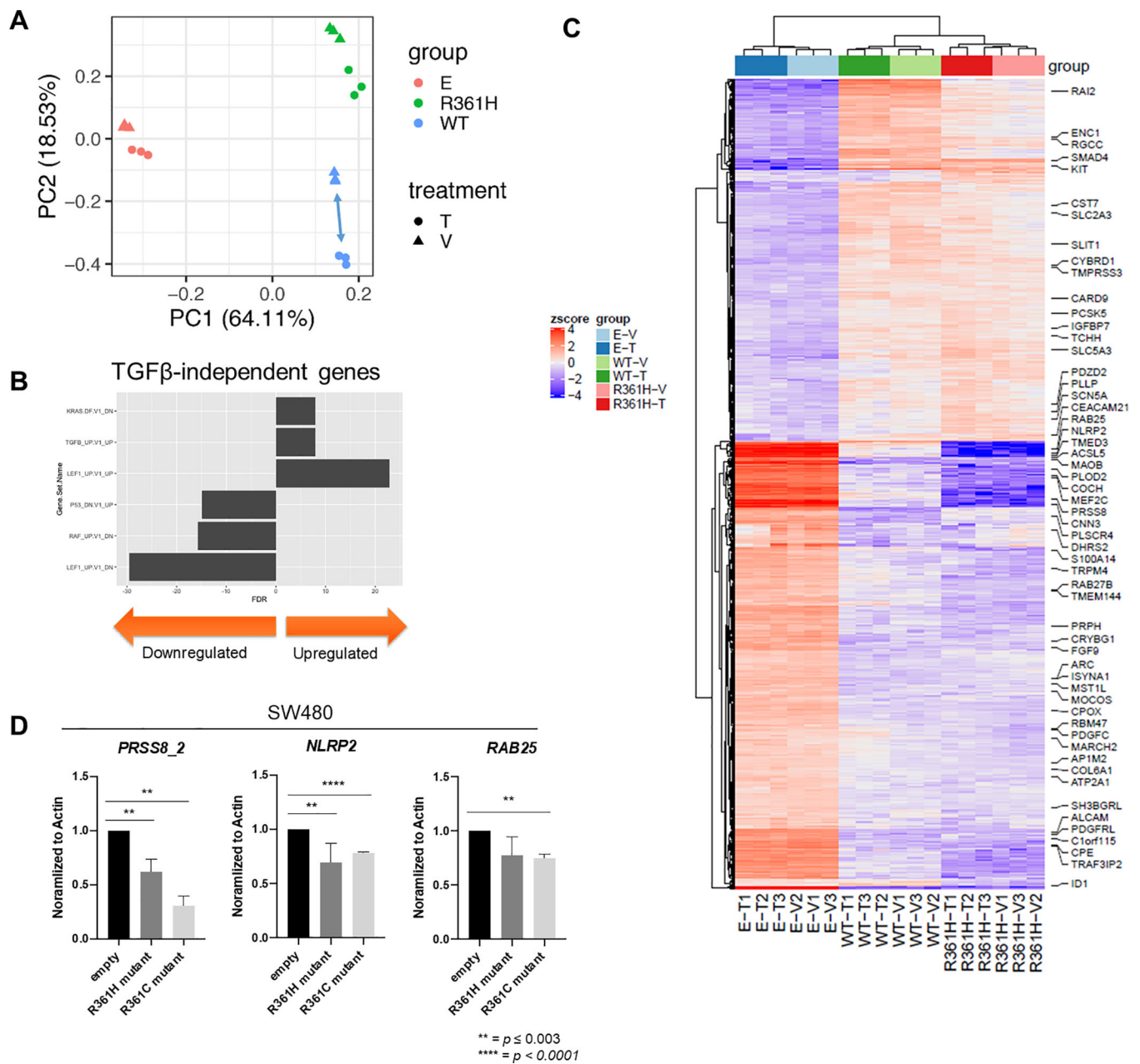


Figure 3. Smad4 R361H mutant confers the gene signature associated with upregulation of the Lef1 transcription factor.

(A) Principal component analysis (PCA) applied to transcriptomes corresponding to indicated treatment groups. (B) Gene Set Enrichment Analysis (GSEA) of pathways enriched in genes differentially expressed in Smad4-R361H vs empty-vector. (C) Heat map representing the transcriptome of CRC cells expressing wtSmad4, the R361H mutant, or empty vector. (D) qRT-PCR validation in SW480 cells of *NLRP2*, *PRSS8* and *RAB25* transcripts. Actin was used as the endogenous control and empty vector cells were used to normalize expression of all three genes.

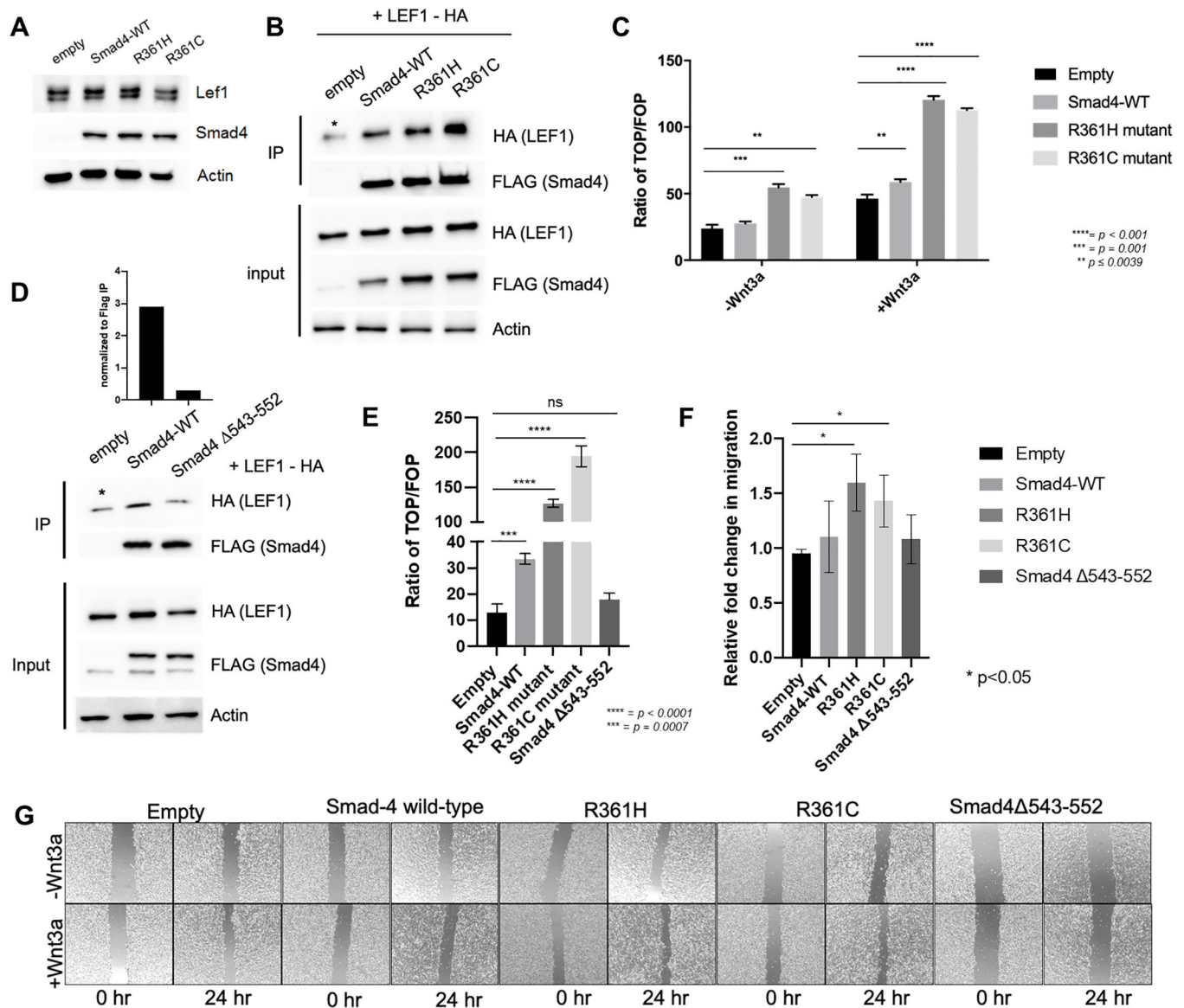


Figure 4. Binding of Smad4 to Lef1 is required for increased WNT signaling.

(A) Western blotting analysis of Lef1 protein levels in SW480 cell derivatives. (B) Analysis of Smad4-Lef1 interactions in HCT116 3:6 cells. Smad4 transduced cells were transfected with Lef1-HA constructs followed 48 hours later by immunoprecipitation with FLAG-conjugated beads. Input/Whole Cell Lysate (WCL) was used as a control. The asterisk here and in D denotes a background band. (C) Analysis of canonical Wnt signaling in HCT116 3:6 cell derivatives. All cultures were transfected with either the TOP-flash or control FOP-flash construct and subsequently treated with either vehicle control or Wnt3a ligand. pRL-TK plasmid was used as an internal control. (D) Analysis of Smad4 $\Delta 543-552$ -Lef1 interactions in HCT116 3:6 cells. Procedures from panel B were followed. Quantitation of Lef1 bands using Image J is shown on top. (E) Analysis of canonical Wnt signaling in Smad4 $\Delta 543-552$ -expressing HCT116 3:6 cells. Procedures from panel C were followed. (F) Quantitation of "wound" closure 24 hours after scratching the monolayer. Bars represent

ratios of cell migration under Wnt3a “+” and “-“ conditions across three independent experiments. (G) Representative images showing migration patterns of HCT116 3:6 cell derivatives.

Author Manuscript

Author Manuscript

Author Manuscript

Author Manuscript

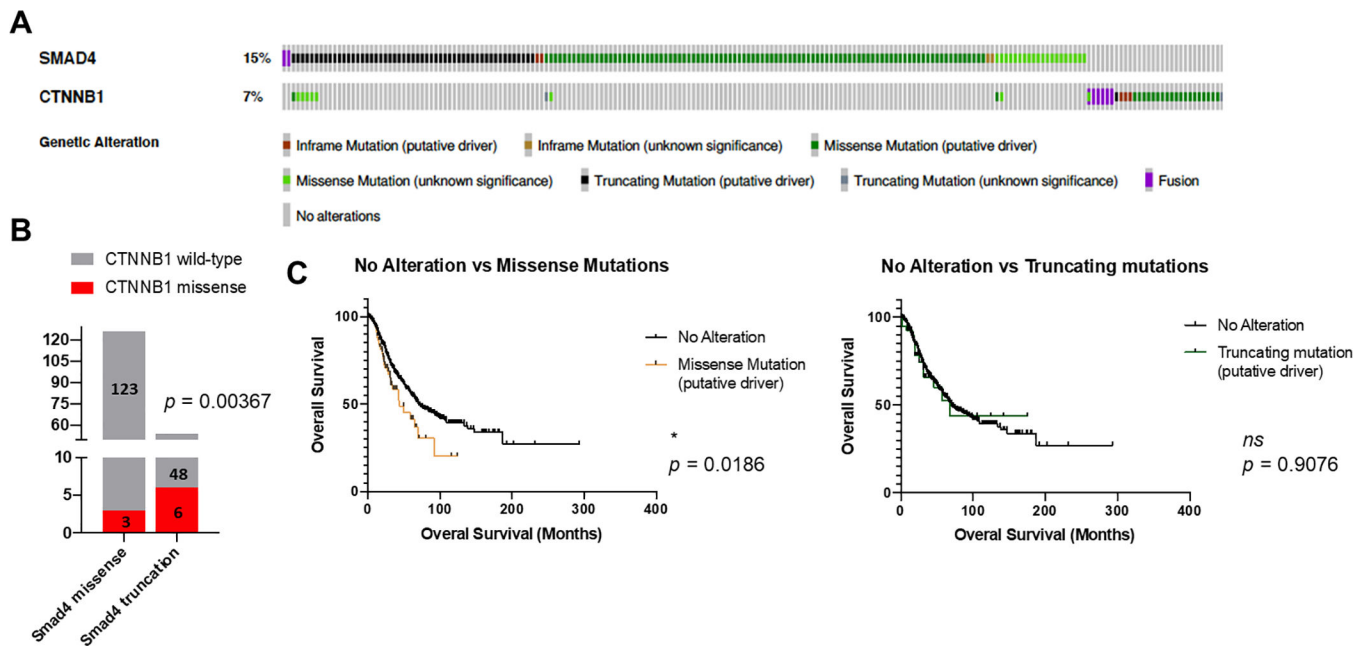


Figure 5. Wnt and TGF β pathway mutations are interdependently distributed in human CRC. (A) Distribution of SMAD4 and CTNNB1 mutations in microsatellite-stable CRC samples. The oncoprint was generated using the cBioPortal for Cancer Genomics. (B) Distribution of missense and truncating nonsense SMAD4 mutations in patients with wild type or mutant CTNNB1. The p-value was calculated using Yate's continuity corrected chi-square test. (C) Kaplan-Meier survival curves corresponding to patients with no SMAD4 alterations and SMAD4 missense (left) and truncating (right) mutations. The p-values were calculated using log-rank Mantel-Cox test.